Supporting Information for

Novel Bimetallic Core–Shell Nanocrystal–Clay Composites with Superior Catalytic Activities

Dharmesh Varade and Kazutoshi Haraguchi*

Material Chemistry Laboratory, Kawamura Institute of Chemical Research, 631 Sakado, Sakura, Chiba 285-0078, Japan.

EXPERIMENTAL SECTION

Materials. An inorganic clay, namely synthetic hectorite (Laponite XLG $[Mg_{5.34}Li_{0.66}Si_8O_{20}(OH)_4]Na_{0.66}$), with a cation-exchange capacity of 104 mequiv/100 g (Rockwood, Ltd., UK) was used after being purified, washed, and vacuum-dried. Analytical-grade ascorbic acid, potassium tetrachloroplatinate(II) (K_2PtCl_4), sodium tetrachloroaurate(III) [$Na(AuCl_4).2H_2O$], 4-nitrophenol, and sodium borohydride ($NaBH_4$) were purchased from Wako Pure Chemical Industries, Ltd. (Japan), and potassium tetrachloropalladate(II) (K_2PdCl_4) was obtained from Alfa Aesar. All of these reagents were used without further purification, unless otherwise stated. Ultrapure water supplied by a PURIC-MX system (Organo Co., Japan) was used for all experiments.

Clay dispersion. Clay swells when dispersed in water and gradually cleaves into discrete disk-like particles of diameter ~30 nm and thickness 1 nm. The clay particle shape is a result of layer packing. A central sheet of O^{2-} and OH^- ions, defining octahedral sites that are occupied by Mg^{2+} ions, is sandwiched between two inverted sheets of tetrahedral silicates. The outer surfaces of these layers therefore comprise oxygen atoms that are involved in siloxane bonds. Hydroxyl groups are present on the edges of the particles. Depending on the pH of the suspension, the edges of the clay particles can be positively charged. In synthetic laponite XLG, the substitution of Li^+ ions for Mg^{2+} ions is the source of the negative charges. Dispersions of these inorganic particles were prepared by adding a known amount of powder to water, with gentle mixing, at 40 °C for 60 min. The resulting aqueous clay dispersion, which consisted of exfoliated clay particles, was homogeneous, transparent, and had a fairly high pH (10.2) and negative zeta potential (−37.1 mV).[20]

Preparation of core–shell nanocrystal/clay composites. Typical syntheses of various bimetallic NCs were performed as follows.

(1) For Pd–Pt core–shell NCs (Pt/Pd molar ratio = 1.0), 1.0 ml of K_2PtCl_4 solution (20 mM) and 1.0 ml of K_2PdCl_4 solution (20 mM) were mixed with 1 ml of clay dispersion (2 wt%) in a glass vial (5 ml).
(2) For Au–Pd core–shell NCs (Au/Pd molar ratio = 1.0), 1 ml of $Na(AuCl_4).2H_2O$ (20 mM) and 1.0 ml of K_2PdCl_4 solution (20 mM) were mixed with 1 ml of clay dispersion (2 wt%) in a glass vial (5 ml).
(3) For Au–Pt core–shell NCs (Au/Pt molar ratio = 1.0), 1 ml of $Na(AuCl_4).2H_2O$ (20 mM) and 1.0 ml of K_2PtCl_4 solution (20 mM) were mixed with 1 ml of clay dispersion (2 wt%) in a glass vial (5 ml).

Subsequently, 0.5 ml of ascorbic acid solution (0.4 M) was quickly added to each vial [(1), (2), and (3)] under sonication at room temperature. After sonication for 10 min, the mixture solution was left for 24 h at room temperature. The product was collected by centrifugation at 10 000 rpm for 10 min and three consecutive washing/centrifugation cycles with water. For further characterization, the collected product was redispersed in water (1 ml) to produce a stable colloidal suspension.

Catalytic reduction of 4-Nitrophenol: A 0.5 mL sample of $NaBH_4$ solution (60 mmol/l) was added to 2.5 ml of 4-nitrophenol solution (0.12 mmol/l) in a glass vessel. A known amount of catalyst was then added and the mixture was stirred. Ultraviolet (UV) spectra of the samples were recorded immediately, and then at 60 s intervals, in the range 250–550 nm at 25 °C.

Characterization. The morphologies of the bimetallic NCs were examined using high-resolution field-emission transmission electron microscopy (TEM; JEM-2200TFE, JEOL) at 200 kV. The sample was prepared by depositing a drop of the dilute sample solution on a carbon-coated Cu grid and drying at room temperature. Energy dispersive X-ray spectroscopy was performed using a scanning TEM detector fitted on a JEOL JEM-2200TFE instrument operated at 200 kV. Wide-angle powder X-ray diffraction patterns were obtained using a Rigaku SmartLab X-ray diffractometer with monochromated Cu Kα radiation (40 kV, 100 mA). X-ray photoelectron spectra were recorded using an ESCALab MKII X-ray photoelectron spectrometer fitted with an Mg Kα radiation excitation source. N_2 adsorption–desorption data were obtained using a BELSORP-mini II (BEL Japan Inc.) instrument operated at −196 °C. Prior to measurements, the sample was added to the measurement cell, which was placed in a drying machine and heated at 80 °C overnight. After drying, helium gas was added to the cell. UV-visible (UV-vis) absorption spectra were recorded with samples in a quartz cuvette (1 mm) at room temperature, using a Hitachi U-4100 UV-vis double-beam spectrometer.

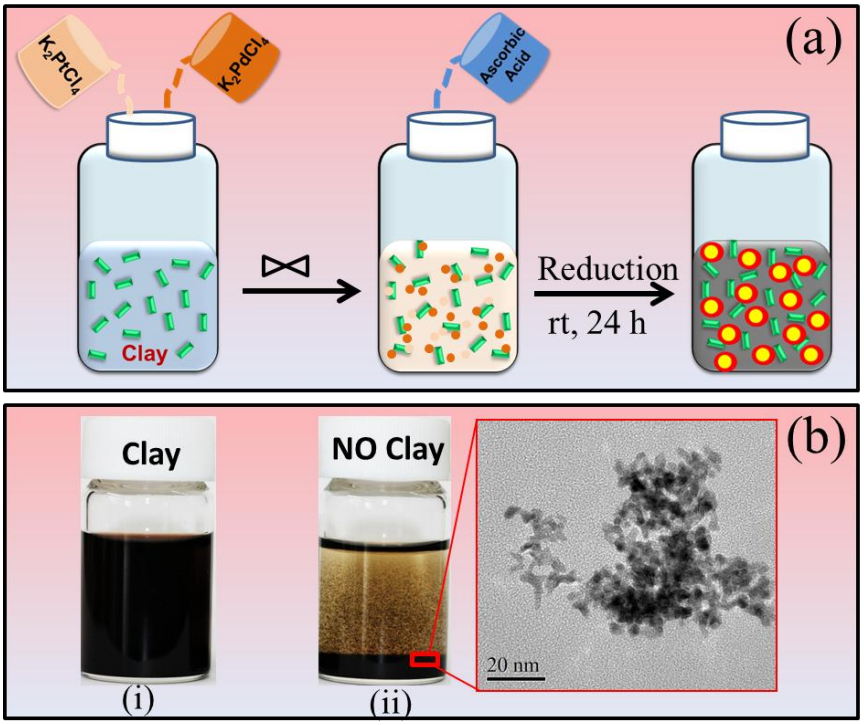

Figure S1: (a) Schematic representation of preparation of Pd–Pt core–shell NCs in presence of clay. (b) Optical images depicting formation of Pd–Pt core–shell NCs in the (i) presence and (ii) absence of clay. Inset shows the corresponding TEM image for the NCs in the absence of clay.

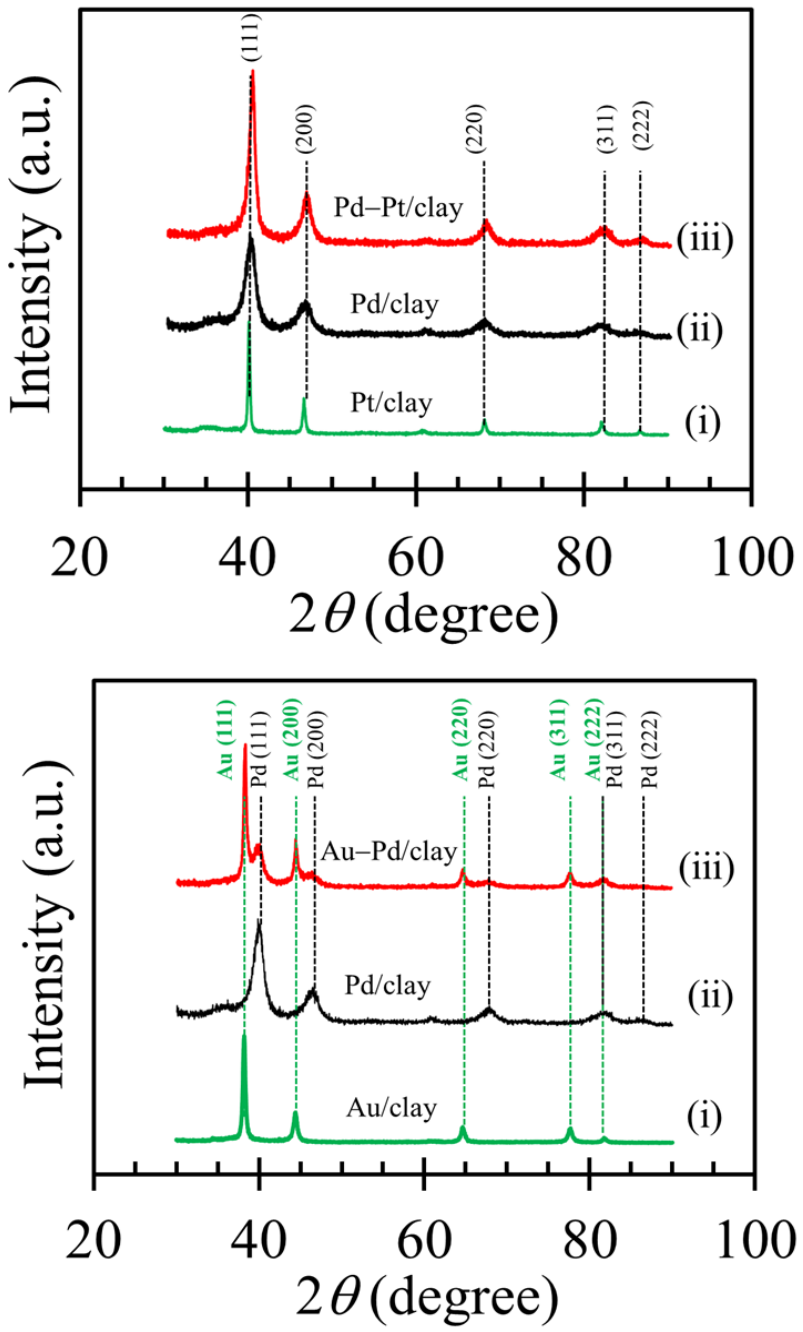

Figure S2: X-ray diffraction patterns of (a) (i) Pt/clay, (ii) Pd/clay, and (iii) Pd–Pt/clay; (b) (i) Au/clay, (ii) Pd/clay, and (iii) Au–Pd/clay.

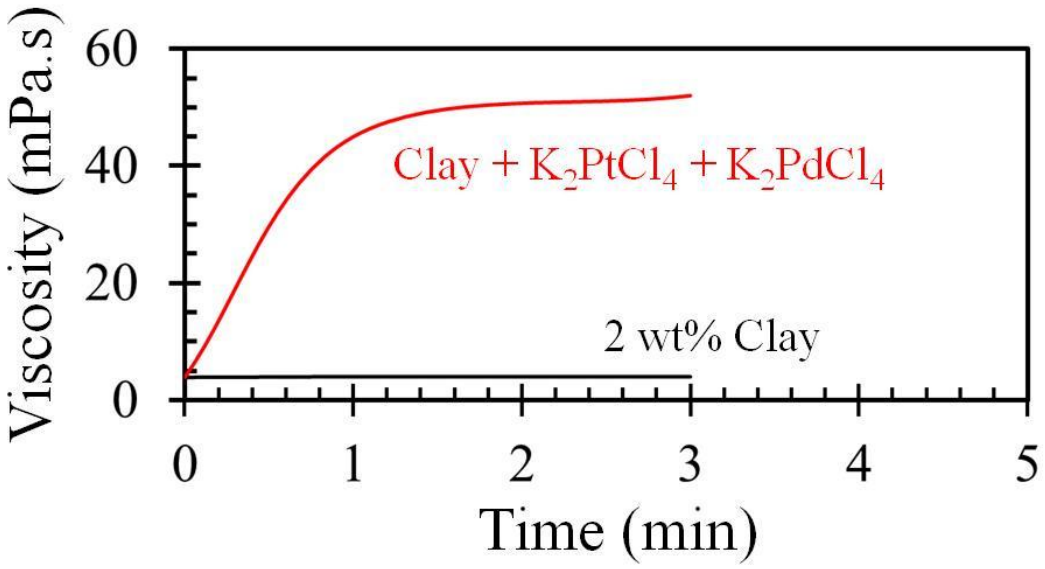

Figure S3: The viscosity change of clay suspension (2 wt%) by addition of K_2PtCl_4 (20 mM) and K_2PdCl_4 (20 mM).

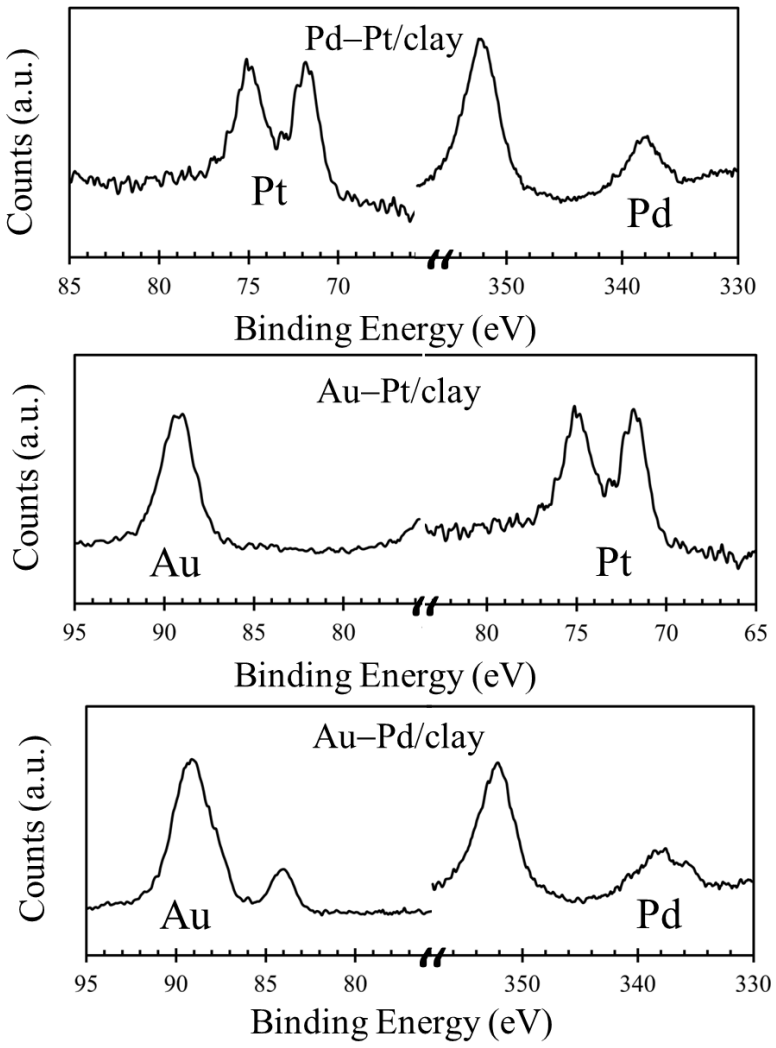

Figure S4: X-ray photoelectron spectra of various core–shell NC/clay composites.

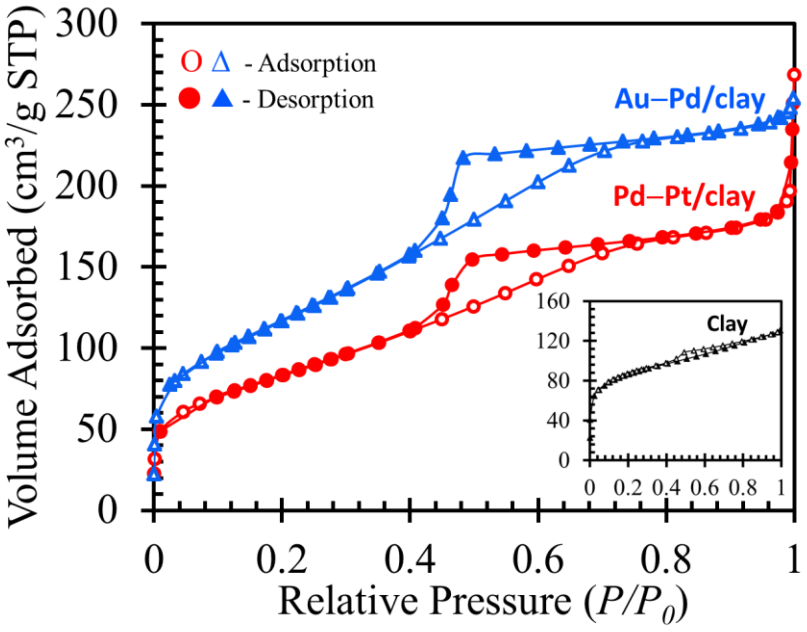

Core–Shell NC/Clay	Surface Area a_s (BET) ($m^2 g^{-1}$)	Average Pore Size (nm)
Clay	314	4.04
Pd–Pt/clay	290.7	4.37
Au–Pd/clay	343.5	4.02

Figure S5: N_2 adsorption–desorption measurements for Pd–Pt/clay and Au–Pd/clay composites. Inset shows corresponding N_2 adsorption–desorption measurements for clean clay. Table illustrates data analysis for N_2 adsorption–desorption measurements.

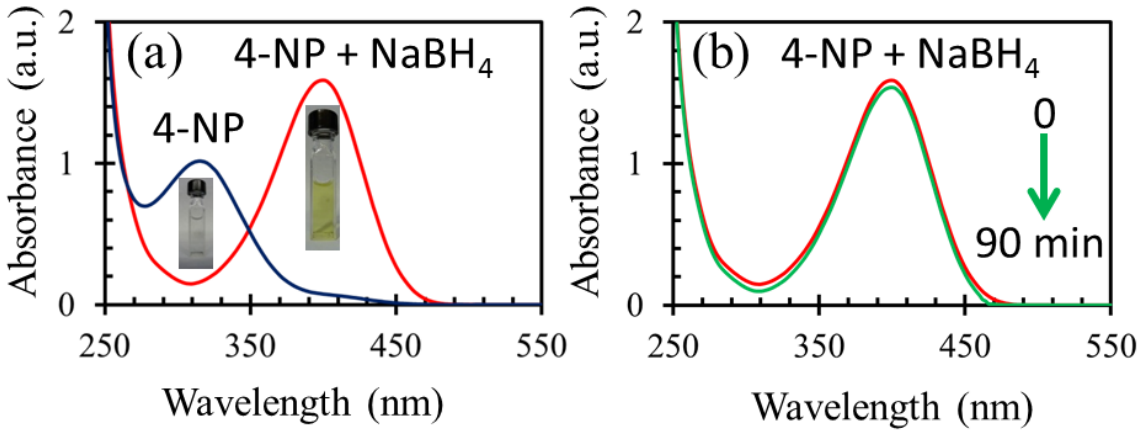

Figure S6: (a) Ultraviolet-visible (UV-vis) spectra of 4-nitrophenol (4-NP) and 4-NP + $NaBH_4$. (b) No change in UV-vis spectrum of 4-NP + $NaBH_4$ after 90 min.

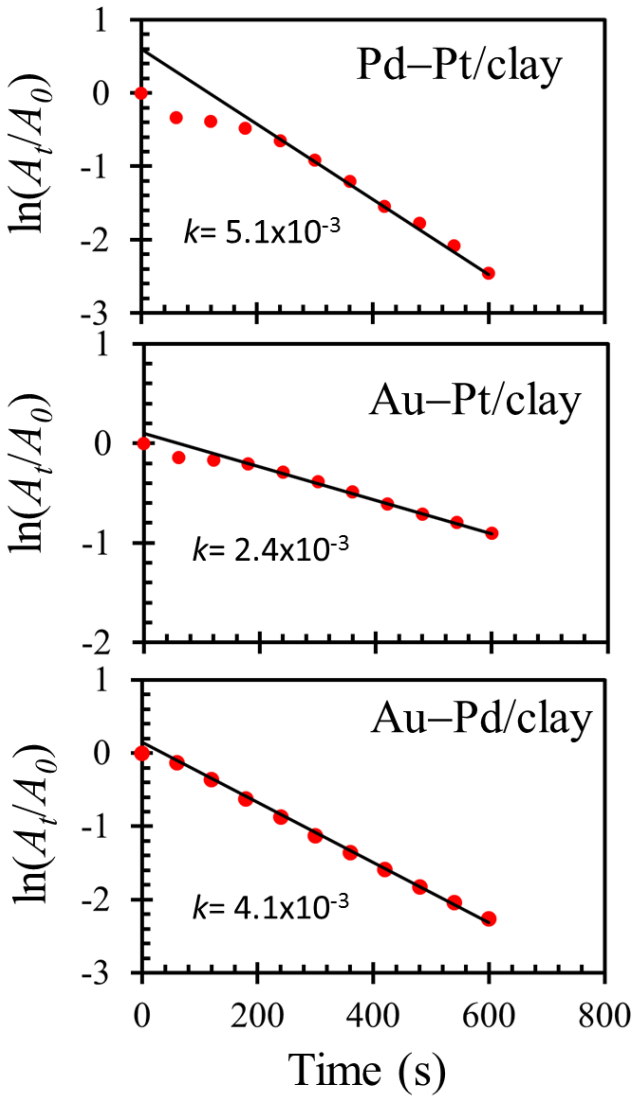

Figure S7: Linear correlation of $\ln(A_t/A_0)$ with time (A_t and A_0 represent the absorbance at time t and of the initial 4-nitrophenolate ions, respectively) for as-prepared core–shell NC/clay composites. Black lines show slopes, which correspond to rate constants (k).